

Exchange Coupling of Transition-Metal Ions through Hydrogen Bonding: A Theoretical Investigation

Cédric Desplanches, Eliseo Ruiz, Antonio Rodríguez-Forteza, and Santiago Alvarez*

Contribution from the Departament de Química Inorgànica, and Centre Especial de Recerca en Química Teòrica (CeRQT), Universitat de Barcelona, Diagonal 647, 08028 Barcelona, Spain

Received December 19, 2001

Abstract: Density functional calculations for full structures of dimers of Cu(II) complexes linked via O—H...O hydrogen bonds provide exchange-coupling constants that are in excellent agreement with experimentally reported values. Magneto-structural correlations between the exchange-coupling constant and the O...O distance or the separation between the coordination planes of the two monomers are analyzed. The calculations support the orbital models usually employed in qualitative interpretations of magneto-structural correlations, showing excellent correlations between the calculated coupling constants and the square of the orbital gap or of the overlap between the two magnetic orbitals. The orbital gap responsible for the antiferromagnetic coupling is seen to result from direct through-space overlap between the oxygen atoms of the two monomers, whereas the hydrogen bonds play an essentially structural role by holding these oxygen atoms in close proximity.

Despite the wealth of theoretical studies and magneto-structural correlations reported in recent years to account for the magnetic exchange coupling between transition-metal ions in dinuclear complexes, these have always referred to systems in which the metal atoms are linked through covalent bonds to bridging ligands,¹ that is, the local spins are coupled through *superexchange* interaction. Intermolecular exchange interaction through hydrogen bonds, on the other hand, has been well documented from the experimental point of view in several cases, including very weak to moderately strong antiferromagnetic interactions. For the case of Cu(II) complexes (Table 1), the formation of hydrogen bonds by equatorial ligands of square pyramids, Jahn–Teller distorted square bipyramids, or square planar complexes results in antiferromagnetic coupling of varying strengths (Table 1, compounds **A–G**), whereas hydrogen bonding connecting an equatorial ligand of one monomer with an axial ligand of another one seems to give a rather weak ferromagnetic coupling (Table 1, compounds **K** and **L**). Although in the present contribution we focus on Cu(II) complexes only, it is worth mentioning that exchange coupling through hydrogen bonding has also been reported for complexes of other transition-metal complexes, notably Cr(III),^{12–17} Fe-

Table 1. Experimental Exchange-Coupling Constants and Oxygen–Oxygen Distances for Dimeric Cu(II) Complexes Linked through Hydrogen Bonding

cmpd	O...O (Å)		J (cm ⁻¹)	refcode	h (Å) ^a	ref
A	2.34	2.34	-94	HEAICU10	0.45, 0.22	2
B	2.45	2.43	-56	AETCUA	1.43, 1.47	3
C	2.52	2.52	-70	AETCUB	1.63, 1.82	3
D	2.48	2.42	-49	FAXGOA	0.64, 1.66	4
E	2.49	2.45	-27	FAXGUG	1.69, 1.97	4
F	2.76	2.76	-4.4	SAGLAC	1.00	5,6
G	2.60		-21		0.06, 1.77 ^b	7
H	2.46		-4.1	PITTAN	1.82	8
I	2.44		+0.06	BOYPIO		9
J	2.50	2.50	"weak"	CUJLEY	0.95, 1.20	10
K	2.66		-7		<i>c</i>	7
L	2.89		+0.3	BEYRAY01		11

^a h is calculated as the distance of the oxygen atom of one monomer relative to the CuO₂N₂ plane of the other monomer, given only for complexes with coplanar basal planes. ^b The basal planes of the two monomers are twisted with respect to each other. ^c One hydrogen bond between basal ligands and two between axial and equatorial ligands.

(II),¹⁸ Fe(III),¹⁹ Ni(II),²⁰ and for a Co(III)/Cr(III) mixed-metal system,²¹ with weak antiferromagnetic interactions in all cases.

* To whom correspondence should be addressed. E-mail: santiago@qi.ub.es.

- Ruiz, E.; Alvarez, S.; Rodríguez-Forteza, A.; Alemany, P.; Pouillon, Y.; Massobrio, C. In *Magnetism: Molecules to Materials*; Miller, J. S., Drillon, M., Eds.; Wiley-VCH: New York, 2001; Vol. 2, pp 227–279.
- Bertrand, J. A.; Black, T. D.; Eller, P. G.; Helm, F. T.; Mahmood, R. *Inorg. Chem.* **1976**, *15*, 2965.
- Bertrand, J. A.; Fujita, E.; Vanderveer, D. G. *Inorg. Chem.* **1980**, *19*, 2022.
- Muhonen, H. *Inorg. Chem.* **1986**, *25*, 4692.
- Estes, W. E.; Hatfield, W. E. *Inorg. Chem.* **1978**, *17*, 3226.
- Ueki, T.; Ashida, T.; Sasada, Y.; Kakudo, M. *Acta Crystallogr., Sect. B* **1969**, *25*, 328.
- Plass, W.; Pohlmann, A.; Rautengarten, J. *Angew. Chem., Int. Ed.* **2001**, *40*, 4207.
- Arulsamy, N.; Glerup, J.; Hodgson, D. J. *Inorg. Chem.* **1994**, *33*, 2066.

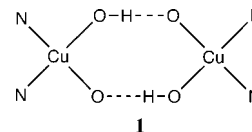
- Nieuwpoort, G.; Verschoor, G. C.; Reedijk, J. *J. Chem. Soc., Dalton Trans.* **1983**, 531.
- Masi, D.; Mealli, C.; Sabat, M.; Sabatini, A.; Vacca, A.; Zanolini, F. *Helv. Chim. Acta* **1984**, *67*, 1818.
- Klein, C. L.; Majeste, R. J.; Trefonas, L. M.; O'Connor, C. J. *Inorg. Chem.* **1982**, *21*, 1891.
- Goodson, P. A.; Glerup, J.; Hodgson, D. J.; Michelsen, K.; Rychlewska, U. *Inorg. Chem.* **1994**, *33*, 359.
- Bossek, U.; Wieghardt, K.; Nuber, B.; Weiss, J. *Angew. Chem., Int. Ed. Engl.* **1990**, *29*, 1055.
- Bossek, U.; Haselhorst, G.; Ross, S.; Wieghardt, K.; Nuber, B. *J. Chem. Soc., Dalton Trans.* **1994**, 2043.
- Goodson, P. A.; Glerup, J.; Hodgson, D. J.; Jensen, N. B.; Michelsen, K. *J. Chem. Soc., Dalton Trans.* **2001**, 2783.
- Ardon, M.; Bino, A.; Michelsen, K.; Pedersen, E. *J. Am. Chem. Soc.* **1987**, *109*, 5855.
- Ardon, M.; Bino, A.; Michelsen, K.; Pedersen, E.; Thompson, R. C. *Inorg. Chem.* **1997**, *36*, 4147.

Since hydrogen bonding is presently one of the best known strategies to build supramolecular arrays in a controlled way, a large effort has been devoted to the understanding of the structural aspects of hydrogen bonding in transition-metal chemistry in regard with the assembly of supramolecular arrays,^{22–25} but little systematic work has been aimed at understanding how the magnetic properties can be controlled through hydrogen bonding. Hence, it is of the utmost importance to understand the mechanism of the magnetic exchange interactions mediated by hydrogen bonding, as well as the factors that determine their strength.

The only theoretical study on the exchange coupling through hydrogen bonds published thus far²⁶ used ab initio calculations with the perturbational methodology proposed by de Loth et al.²⁷ In that study, the effect of the intermolecular O···O distance between two model Cu(II) monomers on the exchange-coupling constant was analyzed. The availability of modern density functionals combined with the broken-symmetry approach has been revealed as a powerful computational technique to obtain good estimates of the exchange-coupling constant in di- and polynuclear transition-metal complexes with a variety of bridging ligands.^{1,28} It thus seems adequate to explore the capability of such a technique to evaluate the exchange coupling through hydrogen bonding and to search for magneto-structural correlations in this field as well as for simple explanations of the coupling mechanism. The use of density functional calculations should allow us to perform a much wider computational study than the ab initio one previously reported, including calculations for full unmodeled structures.

As a first step in the study of hydrogen-bonded complexes we choose the family of Cu(II) compounds with the general topology represented in **1**, which is found in complexes **A–G** (Table 1) with an additional axial ligand on each Cu atom, and in complex **H** with the same square planar coordination sphere represented in **1**. In other molecular topologies found, a hydrogen bond may link equatorial and axial positions (compounds **K** and **L**), or two equatorial planes are oriented nearly perpendicular to each other rather than being coplanar (compound **I**). We report first calculations of the exchange-coupling constant for the unmodeled structures and compare the results with the experimental data. We will then analyze the effect of three structural factors on the exchange coupling in the prototype compound **A**: (a) the O···O distance, (b) the symmetric or asymmetric position of the hydrogen between the two oxygen atoms, and (c) the distance between the two CuN₂O₂ coordination planes at constant O···O distance. Molecular orbital explanations will be sought after, discussing the relationship of

the exchange-coupling constant with the energy gap between the partially occupied molecular orbitals or with the overlap between the magnetic orbitals. Finally, we will discuss the calculated spin population distribution both in the monomer and in the dimer of **A**.



Computational Methodology

The computational strategy adopted in previous theoretical studies on exchange-coupled dinuclear complexes²⁹ has been used. For the evaluation of each coupling constant, two separate DFT calculations³⁰ are carried out, one for the highest spin state and another one for a broken-symmetry singlet state. The hybrid B3LYP method³¹ has been used in all calculations as implemented in Gaussian-98,³² mixing the exact Hartree–Fock exchange with Becke’s expression for the exchange³³ and using the Lee–Yang–Parr correlation functional.³⁴ We have previously found that, among the most common functionals, the B3LYP method combined with the broken-symmetry^{35–38} treatment provides the best results for calculating coupling constants.²⁹ For the Cu atoms a basis set of triple- ζ quality³⁹ was used for the valence orbitals supplemented with two p orbitals (“polarization functions”), whereas a double- ζ basis set⁴⁰ was used for C, H, N, and O atoms, supplemented for the atoms involved in hydrogen bonding with a polarization function (H) and a polarization and a diffuse functions (O). For the estimation of the interaction energy between two monomers, the basis set superposition error was corrected by means of the counterpoise method.⁴¹

We evaluate the coupling constant J from the calculated energies of the high-spin (triplet) and broken-symmetry states according to the following expression:

$$J = \frac{2(E_{\text{BS}} - E_{\text{HS}})}{S(S + 1)} \quad (1)$$

where S is the total spin for the high-spin state and E_{BS} and E_{HS} are the calculated energies for the broken-symmetry and high-spin states, respectively. Such a formula is not spin-projected and assumes that the energy of the singlet state is adequately simulated by that of the

- (18) Garge, P.; Chikate, R.; Padhye, S.; Savariault, J.-M.; de Loth, P.; Tuchagues, J.-P. *Inorg. Chem.* **1990**, *29*, 3315.
 (19) De Munno, G.; Ventura, W.; Viau, G.; Lloret, F.; Faus, J.; Julve, M. *Inorg. Chem.* **1998**, *37*, 1458.
 (20) Figgis, B. N.; Kennedy, B. J.; Murray, K. S.; Reynolds, P. A.; Wright, S. *Austr. J. Chem.* **1982**, *35*, 1807.
 (21) Figgis, B. N.; Kucharski, E. S.; Vrtis, M. *J. Am. Chem. Soc.* **1993**, *114*, 176.
 (22) Desiraju, G. R. *J. Chem. Soc., Dalton Trans.* **2000**, 3745.
 (23) Desiraju, G. R.; Steiner, T. *The Weak Hydrogen Bond in Structural Chemistry and Biology*; Oxford University Press: Oxford, 1999.
 (24) Moulton, B.; Zaworotko, M. J. *Chem. Rev.* **2001**, *101*, 1629.
 (25) Beatty, A. M. *CrystEngComm* **2001**, *1*, 51.
 (26) Nepveu, F.; Gehring, S.; Walz, L. *Chem. Phys. Lett.* **1986**, *128*, 300.
 (27) de Loth, P.; Cassoux, P.; Daudey, J. P.; Malrieu, J. P. *J. Am. Chem. Soc.* **1981**, *103*, 4007.
 (28) Ruiz, E.; Rodríguez-Fortea, A.; Alemany, P.; Alvarez, S. *Polyhedron* **2001**, *20*, 1323.

- (29) Ruiz, E.; Alemany, P.; Alvarez, S.; Cano, J. *J. Am. Chem. Soc.* **1997**, *119*, 1297.
 (30) Parr, R. G.; Yang, W. *Density-Functional Theory of Atoms and Molecules*; Oxford University Press: New York, 1989.
 (31) Becke, A. D. *J. Chem. Phys.* **1993**, *98*, 5648.
 (32) Frisch, M. J.; Trucks, G. W.; Schlegel, H. B.; Scuseria, G. E.; Robb, M. A.; Cheeseman, J. R.; Zakrzewski, V. G.; Montgomery, J. A.; Stratmann, R. E.; Burant, J. C.; Dapprich, S.; Millam, J. M.; Daniels, A. D.; Kudin, K. N.; Strain, M. C.; Farkas, O.; Tomasi, J.; Barone, V.; Cossi, M.; Cammi, R.; Mennucci, B.; Pomelli, C.; Adamo, C.; Clifford, S.; Ochterski, J.; Petersson, G. A.; Ayala, P. Y.; Cui, Q.; Morokuma, K.; Malick, D. K.; Rabuck, A. D.; Raghavachari, K.; Foresman, J. B.; Cioslowski, J.; Ortiz, J. V.; Stefanov, B. B.; Liu, G.; Liashenko, A.; Piskorz, P.; Komaromi, I.; Gomperts, R.; Martin, R. L.; Fox, D. J.; Keith, T.; Al-Laham, M. A.; Peng, C. Y.; Nanayakkara, A.; Gonzalez, C.; Challacombe, M.; Gill, P. M. W.; Johnson, B. G.; Chen, W.; Wong, M. W.; Andres, J. L.; Head-Gordon, M.; Replogle, E. S.; Pople, J. A. *Gaussian 98, Revision A.7*; Gaussian, Inc.: Pittsburgh, PA, 1998.
 (33) Becke, A. D. *Phys. Rev. A* **1988**, *38*, 3098.
 (34) Lee, C.; Yang, W.; Parr, R. G. *Phys. Rev. B* **1988**, *37*, 785.
 (35) Noodleman, L. *J. Chem. Phys.* **1981**, *74*, 5737.
 (36) Noodleman, L.; Davidson, E. R. *Chem. Phys.* **1986**, *109*, 131.
 (37) Noodleman, L.; Case, D. A. *Adv. Inorg. Chem.* **1992**, *38*, 423.
 (38) Noodleman, L.; Peng, C. Y.; Case, D. A.; Mouesca, J. M. *Coord. Chem. Rev.* **1995**, *144*, 199.
 (39) Schaefer, A.; Huber, C.; Ahlrichs, R. *J. Chem. Phys.* **1994**, *100*, 5829.
 (40) Schaefer, A.; Horn, H.; Ahlrichs, R. *J. Chem. Phys.* **1992**, *97*, 2571.
 (41) Boys, S. F.; Bernardi, F. *Mol. Phys.* **1970**, *19*, 553.

Table 2. Calculated and Experimental Exchange-Coupling Constants (cm^{-1}) for Cu(II) Complexes Connected through Hydrogen Bonds

compd	J_{calc}	J_{exp}	topology	ref
A	-87	-94	eq-eq	2
B	-38	-56	eq-eq	3
C	-24	-70	eq-eq	3
D	-42	-49	eq-eq	4
E	-32	-27	eq-eq	4
F	-13	-4.4	eq-eq	5
G ^a	-17	-21	eq-eq	7
K ^a	-6	-7	ax-eq + eq-eq	7
L	-0.02	+0.33	ax-eq	11

^a B3LYP calculated values for G and K from Plass et al.⁷

broken-symmetry state from density functional calculations, in contrast to the criterion adopted by other authors. For a discussion of the relationship between E_{BS} and the energy of the singlet state, the reader is referred to recent papers by us and other authors.^{42,43}

Results for Full Structures

The calculated coupling constants for the unmodeled structures are presented in Table 2. It can be seen that there is a very good agreement between calculated and experimental values of J , except for compound C, for which the calculated antiferromagnetic coupling is consistent with the experimental behavior, although the magnitude is not well reproduced. We defer a discussion of the factors that make the coupling constant vary from one compound to another to a subsequent section, after analyzing the effect of structural parameters on the exchange interaction of the same compound. It is worthy of note that both experiment and computations agree that all Cu(II) compounds that are connected by hydrogen bonding through coplanar equatorial ligands have negative J values characteristic of antiferromagnetic coupling. In contrast, in compound L an equatorial ligand is hydrogen-bonded to an axial ligand, and the compound has been found to be practically uncoupled, with J values of +0.3 and -0.02 cm^{-1} from experiment and theory, respectively. A discussion of the orbital explanation for the antiferromagnetic coupling found in compound A will be given in a later section.

Comparison of the calculated energy for dimer A with the energies of the corresponding monomers gives an interaction energy of 54.5 kcal/mol, which amounts to some 27 kcal/mol per hydrogen bond, a quite large value that probably includes some electrostatic contribution in addition to the hydrogen bond and is only comparable to that calculated for the $\text{H}_2\text{O}\cdots\text{H}_3\text{O}^+$ interaction (32.9 kcal/mol).⁴⁴

The strongest antiferromagnetic coupling between two copper (II) ions attributed to hydrogen bonding has been reported for the chain compound $[\text{Cu}_2(\mu\text{-bpm})_2(\text{H}_3\text{O}_2)(\text{H}_2\text{O})_2]^{3+}$ (bpm is bipyrimidine and H_3O_2^- is the bihydroxide anion formed by hydrogen-bonded OH^- and H_2O), which was reported to be diamagnetic at room temperature (i.e., $J < -600 \text{ cm}^{-1}$).⁴⁵ Since such a strong antiferromagnetic coupling through hydrogen

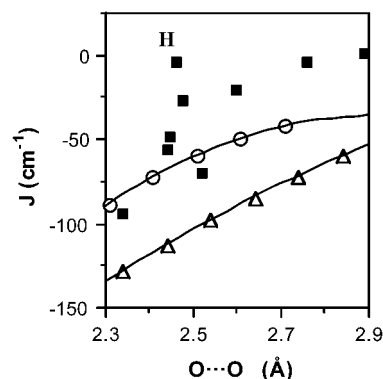


Figure 1. Calculated exchange-coupling constant J as a function of the $\text{O}\cdots\text{O}$ distance for the model compound **1** (open circles) in a coplanar arrangement, together with the values calculated by Nepveu et al.²⁶ (open triangles) and experimental coupling constants (solid squares) from Table 1.

bonding seems unlikely according to the results of Figure 1, we are currently reinvestigating such compound from both the theoretical and experimental sides.⁴⁶

Structural Effects

The effect of the hydrogen-bond distance has been studied by artificially changing the intermolecular distance of compound A, and the results are presented in Figure 1 (open circles) where a parabolic dependence of J on the $\text{O}\cdots\text{O}$ distance is evident. Such a dependence is consistent with the variation of the overlap between the SOMOs of the monomers with the intermolecular distance, as will be discussed in a later section. The ab initio results reported by Nepveu et al.,²⁶ also shown in Figure 1 (open triangles), present the same trend but more negative values. The experimental coupling constants for compounds A–I as a function of the $\text{O}\cdots\text{O}$ distance are plotted alongside the calculated curve (Figure 1, filled squares). These points roughly reproduce the theoretical trend, with the J value becoming less negative as the $\text{O}\cdots\text{O}$ distance increases, although the match is not very good, reflecting differences in molecular structures and the fact that the monomers are not coplanar as assumed in our model calculations, a matter that will be addressed below. In particular, we note that the strong deviation of compound H from the expected behavior is not because it is the only tetracoordinated complex but because it is associated with the large interplanar distance (1.8 Å) between the monomers.

Another structural parameter that we have investigated is the position of the hydrogen between the two oxygen atoms. In this point, a theoretical evaluation is of great interest since in many cases the position of the hydrogen atom is not well established from the X-ray diffraction structure. If the hydrogen atoms in compound A are displaced from their position in the crystal structure to the center of the $\text{O}\cdots\text{O}$ vectors, the calculated coupling constant is not significantly affected (it decreases by only 2 cm^{-1}), a result that will be better understood after the discussion of the orbital analysis below.

Finally, we have analyzed the effect of a vertical separation of the two monomers (h in **2**) on the exchange-coupling constant. This has been done in two different ways, keeping in both cases the $\text{O}\cdots\text{O}$ distances constant ($\text{O}-\text{O} = 2.307 \text{ Å}$, $\text{O}-\text{H} =$

(42) Caballol, R.; Castell, O.; Illas, F.; Moreira, I. d. P. R.; Malrieu, J. P. *J. Phys. Chem. A* **1997**, *101*, 7860.

(43) Ruiz, E.; Cano, J.; Alvarez, S.; Alemany, P. *J. Comput. Chem.* **1999**, *20*, 1391.

(44) Tuma, C.; Boese, A. D.; Handy, N. C. *Phys. Chem. Chem. Phys.* **1999**, *1*, 3939.

(45) De Munno, G.; Viterbo, D.; Caneschi, A.; Lloret, F.; Julve, M. *Inorg. Chem.* **1994**, *33*, 1585.

(46) Desplanches, C.; Ruiz, E.; Lloret, F.; Julve, M.; De Munno, G.; Alvarez, S. Manuscript to be submitted.

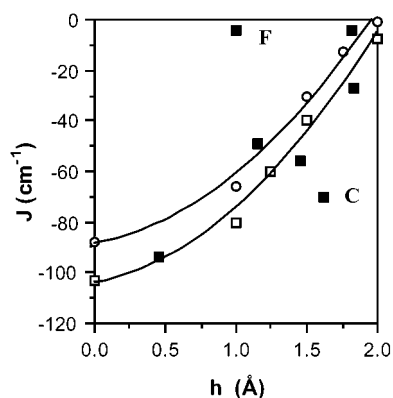
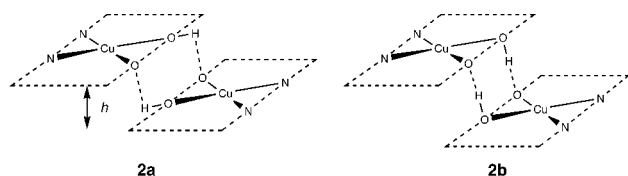


Figure 2. Calculated exchange-coupling constant J as a function of the distance between the coordination planes of the two monomers in the model dimer **1**, keeping the hydrogen atoms in the molecular plane (open circles) and aligning them with the O...O vector (open squares). Experimental coupling constants (solid squares) also shown for comparison.

1.067 Å), either keeping each hydrogen atom in the plane of the monomer to which it is bonded (Figure 2, open circles) as schematically depicted in **2a**, or placing the hydrogen atom along the O–O direction (Figure 2, open squares) as in **2b**. It is found that for all interplanar distances, the most stable geometry is that in which each H is aligned with the hydrogen-bonded oxygen atoms (by up to 50 kcal/mol at an interplanar separation of 2.0 Å). The calculated coupling constant is made less negative as the distance between the coordination planes of the two monomers increases. It can also be seen that for a given interplanar distance the coupling is always more antiferromagnetic if the hydrogen is aligned with the two oxygen atoms. The experimental data are also plotted in Figure 2 (filled squares), where two points are seen to deviate from the theoretically expected behavior. One of them can be explained because the O...O distance (2.76 Å, compound **F**) is much larger than in our calculations (2.31 Å). The other outlier is compound **C**, for which the experimental coupling constant seems to be too antiferromagnetic for the interplanar distance corresponding to such a structure, and we recall that the experimental value is also in disagreement with that calculated for its full structure (Table 2), which is nevertheless consistent with the theoretical magneto-structural correlation of Figure 2. Finally, we note that compound **H**, which did not show the expected relationship between the O...O distance and the experimental J , presents a coupling constant that is in excellent agreement with the expectations for its interplanar distance.



Orbital Analysis of the Exchange Interaction

Since these compounds can be described as two independent monomers interacting weakly through hydrogen bonds, they provide a good case study for an evaluation of the currently applied orbital models of the exchange interaction. One of them, proposed by Hay–Thibeault–Hoffmann,⁴⁷ predicts that the

(47) Hay, P. J.; Thibeault, J. C.; Hoffmann, R. *J. Am. Chem. Soc.* **1975**, *97*, 4884.

antiferromagnetic contribution to the coupling constant depends on the square of the orbital gap according to eq 2, where K_{ab} , J_{aa} , and J_{ab} are the exchange and Coulombic integrals involving orthogonal localized orbitals a and b , and ϵ_1 and ϵ_2 are the energies of the singly occupied, delocalized molecular orbitals (SOMOs) in the triplet state. Another model proposed by Kahn and co-workers^{48–54} results in an expression of J dependent on the overlap between nonorthogonal localized *magnetic* orbitals (eq 3).

$$E_S - E_T = J = 2K_{ab} - \frac{(\epsilon_1 - \epsilon_2)^2}{J_{aa} - J_{ab}} \quad (2)$$

$$J = J_F + J_{AF} \approx 2K_{ab} + 4(\epsilon_1 - \epsilon_2)S_{ab} \quad (3)$$

Although such expressions have been deduced within the framework of the restricted Hartree–Fock theory, it has been shown that the unrestricted Kohn–Sham orbitals obtained from density functional calculations are physically sound and suitable for qualitative molecular orbital theory.^{55,56} Therefore, we adopt an empirical criterion and look for the possible existence of relationships analogous to those in eqs 2 and 3 among the results of our DFT calculations. However, before so doing, it is convenient to clarify the differences expected in orbital composition for the different computational approaches used: restricted, unrestricted, and unrestricted broken symmetry. In restricted calculations, the same orbital is used for a spin-up and a spin-down electron, so that only two molecular orbitals are required for a dimer of a Cu(II) complex, the *singly occupied molecular orbitals* in a triplet state, referred to as the SOMOs of the dimer (Figure 3, upper panel). In an unrestricted calculation for a triplet state, in contrast, the molecular orbitals for the α and β electrons are allowed to be different, and the differences in localization throughout the molecule (usually referred to as *spin polarization*) found in those calculations are associated with the maximization of the exchange interaction and the minimization of the Coulombic interelectronic repulsions. In particular, in the present case, the α orbitals are less localized at the metal atoms than the restricted SOMOs, whereas the corresponding β orbitals are more localized than the SOMOs (Figure 3, middle panel). To differentiate the unrestricted from the restricted orbitals, we term the former *magnetic spin-orbitals*, since the qualifier *magnetic* applied to orbitals has a wide acceptance as meaning the orbitals that describe the unpaired electrons which determine the magnetic behavior of the molecule. Hence, for the triplet state of a dinuclear Cu(II) compound we have two *occupied magnetic spin-orbitals* (OMSOs) corresponding to α electrons and two *unoccupied magnetic spin-orbitals* (UMSOs) with β spin (Figure 3, middle panel). Correspondingly, in the singlet state the two OMSOs correspond to one α and one β electron and in a similar fashion for the two UMSOs.

(48) Girerd, J. J.; Journaux, Y.; Kahn, O. *Chem. Phys. Lett.* **1981**, *82*, 534.

(49) Kahn, O. *Molecular Magnetism*; VCH: New York, 1993.

(50) Kahn, O.; Charlot, M. F. *Nouv. J. Chim.* **1980**, *4*, 567.

(51) Kollman, C.; Kahn, O. *Acc. Chem. Res.* **1993**, *26*, 259.

(52) Kahn, O. *Angew. Chem., Int. Ed. Engl.* **1985**, *24*, 834.

(53) Kahn, O.; Briat, B. *J. Chem. Soc., Faraday Trans. 2* **1976**, *72*, 1441.

(54) Kahn, O.; Briat, B. *J. Chem. Soc., Faraday Trans. 2* **1976**, *72*, 268.

(55) Baerends, E. J.; Gritsenko, O. V. *J. Phys. Chem. A* **1997**, *101*, 5383.

(56) Stowasser, R.; Hoffmann, R. *J. Am. Chem. Soc.* **1999**, *121*, 3414.

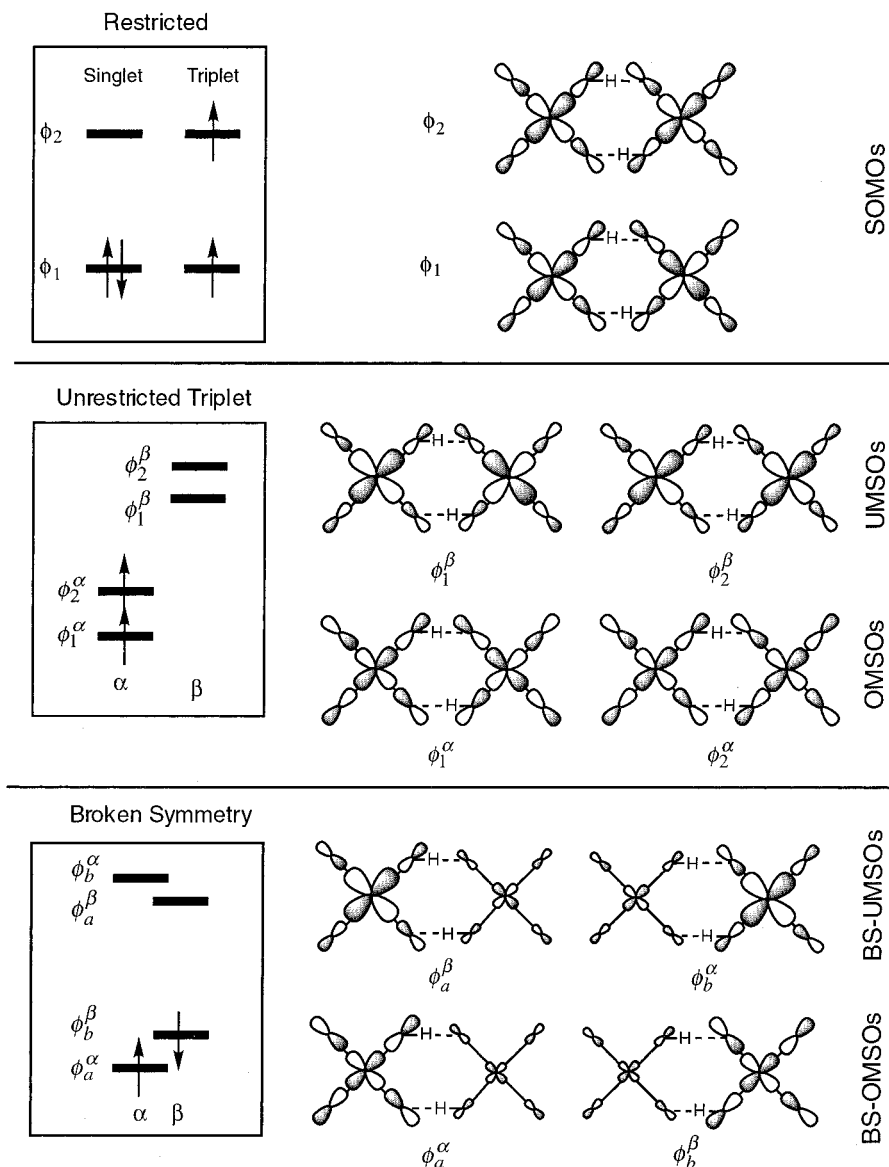
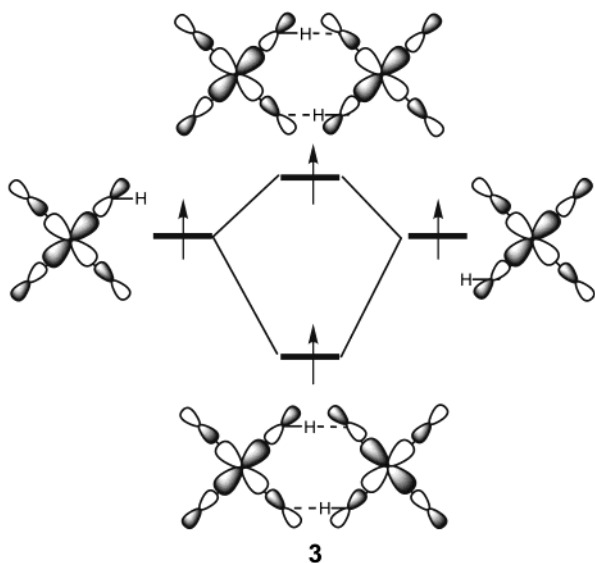


Figure 3. Schematic representation of the singly occupied molecular orbitals (restricted calculations, upper panel), magnetic spin-orbitals (unrestricted calculations, middle panel), and broken-symmetry magnetic spin-orbitals (lower panel) of a dimer of a Cu(II) complex.



The UMSOs of the triplet in compound **A** actually found in our calculations (schematically shown in Figure 3, middle panel) present only a minute contribution at the hydrogen atoms that form hydrogen bonds, and a similar situation is found in the SOMOs of the independent monomers. Despite the almost negligible contribution of the hydrogen atoms to the SOMOs, these $d_{x^2-y^2}$ -type molecular orbitals of the two monomers interact, forming bonding and antibonding combinations (schematically shown in 3, where the simpler restricted approach is assumed for simplicity, showing identical orbitals for the α and β electrons) separated by a substantial gap (ca. 3000 cm^{-1} between the OMSOs of the triplet state), apparently due to through-space O...O interaction. The localization of the SOMOs in the xy plane also explains why a hydrogen bond involving an axial ligand (compound **L**, Tables 1 and 2) results in a practically uncoupled dimer.

If we now allow for symmetry-breaking to have a good estimate of the energy of the singlet state, the spin-orbitals can mix, producing localized (broken-symmetry) versions

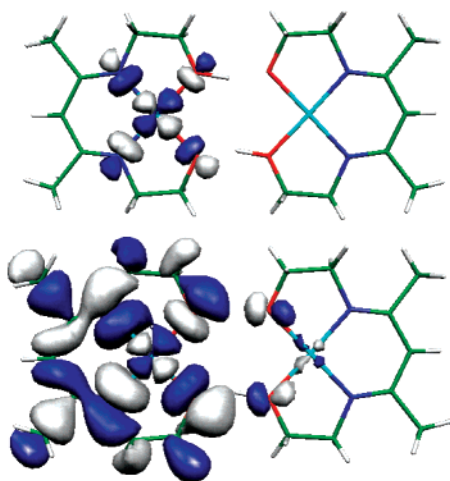
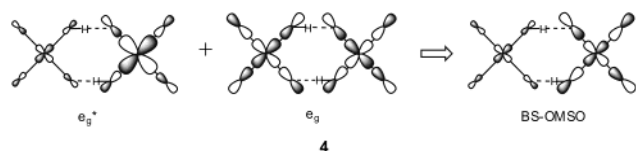


Figure 4. One of the broken-symmetry occupied magnetic spin-orbital (BS-OMSOs) of compound **A** in a coplanar arrangement, represented with two different contours to show the basic shape and localization at one monomer (above) and the small remnant contributions at the other monomer (below).

referred to as BS-OMSOs and BS-UMSOs (schematically represented in Figure 3, lower panel). The corresponding orbitals obtained in our calculations (one of the BS-OMSOs is represented in Figure 4) are strongly localized at one monomer (Figure 4, above), but a small contribution is left at the other monomer. An intriguing result is that such a small contribution has metal–ligand bonding character rather than the usual antibonding one found in all other cases. This is seen to be due to mixing with the low-lying bonding orbital, as schematically represented in **4**, probably as a means of decreasing the Coulomb repulsion with the doubly occupied d orbitals.



To evaluate the existence of a relationship analogous to that of eq 3 among the results of our DFT calculations, we have a choice of possible *magnetic orbitals* to calculate the overlap integral S_{ab} . The obvious choice is to use the singly occupied (α) orbitals of the two monomers. However, in the case of dinuclear complexes with bridging ligands we cannot split the molecule into two independent, chemically meaningful monomers, and the use of the broken-symmetry orbitals of the whole dinuclear entity seems to be a more general approach. Furthermore, it is frequently found in unrestricted DFT calculations that the BS-OMSOs are not very well localized at the metal atoms due to mixing with low-lying orbitals. Hence, we present in Figure 5 the values of J in both geometries, **2a** and **2b**, calculated at different interplanar separations as a function of the overlap integral between the SOMOs of the monomer and between the broken-symmetry orbitals of the dimer (Table 3). It can be seen that in all cases a stronger antiferromagnetic coupling is expected as the overlap between the magnetic orbitals increases. Another important feature shown in Figure 5 is that the relationship between overlap and coupling constant seems to follow a clearer trend when the overlap between the

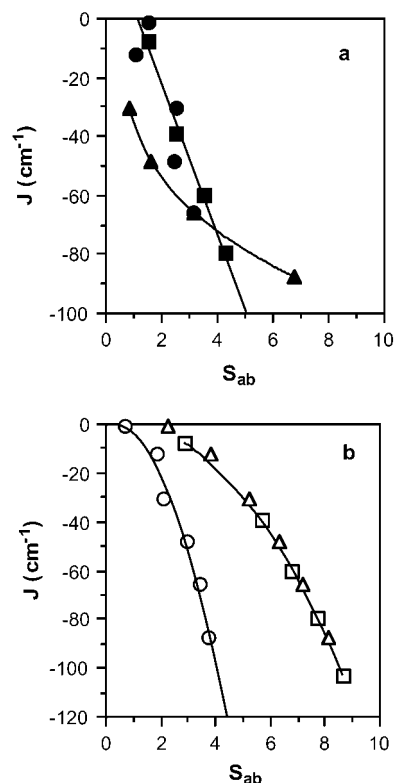


Figure 5. Dependence of the calculated exchange-coupling constant J of compound **A** on the overlap integral ($\times 100$) between (a) occupied magnetic orbitals (solid symbols) of the monomers (circles), BS-OMSOs of the dimer in **2a** (triangles), or BS-OMSOs in **2b** (squares), and (b) between empty magnetic orbitals (open symbols) of the monomers (circles), BS-UMSOs of the dimer in **2a** (triangles), or BS-UMSOs in **2b** (squares).

empty UMSO orbitals is considered, a fact that is associated with a better correlation between the corresponding overlap integrals and the interplanar separation h . In particular, we note that the same dependence of J on S_{ab} (BS-UMSOs) is found, regardless of the position of the hydrogen atoms relative to the oxygen donors and acceptors, in good agreement with the negligible contribution of these hydrogen atoms to the magnetic orbitals. The ill behavior of the overlap between occupied orbitals has been found to be due to their mixing with other occupied α orbitals. These observations are of practical importance, since in many instances the occupied BS-OMSOs are extensively mixed with low-lying orbitals of the same symmetry, making the active electron approximation unpractical. The fact that the overlap between the two BS-UMSOs is larger than that between the BS-OMSOs is due to a lesser localization of the former, thus leaving a residual contribution at one of the monomers; even if its participation is very small, the self-overlap integral between the $d_{x^2-y^2}$ orbital at a given Cu atom in the two BS-UMSOs ($S_{\mu\mu} = 1$) is much larger than, for example, the overlap between the oxygen atoms in two different monomers, and its contribution to the overall overlap becomes significant despite the small coefficient. We also stress that extrapolation of the different curves in Figure 5 to zero overlap predict that only weak ferromagnetic coupling can be expected for these complexes (of $+30 \text{ cm}^{-1}$ at most). In summary, the BS-UMSOs provide an excellent computational version of the *magnetic orbitals* of Kahn–Briat’s model (eq 3), as previously noted by Blanchet-Boiteux and Mouesca⁵⁷ and by us⁵⁸ for other Cu(II) systems (Table 3).

Table 3. Calculated Coupling Constant (cm^{-1}) for Compound **A** at Different Interplanar Separations (h in Å), Together with the Overlap Integrals ($S_{\text{ab}} \times 100$, Absolute Value) between the BS-OMSOs (shown in Figure 4) and BS-UMSOs of the Dimer, Together with the Energy Gap ($\epsilon_1 - \epsilon_2$, cm^{-1}) between the OMSOs or UMSOs of the Triplet State

h	geom.	J_{calc}	S_{ab}		$\epsilon_1 - \epsilon_2$	
			BS-OMSO	BS-UMSO	OMSO	UMSO
0.00	2a	-87.6	6.765	8.144	3024	2258
	2b	-103.4	8.561	8.678	3024	2482
1.00	2a	-65.8	3.159	7.210	3193	1940
	2b	-80.0	4.304	7.716	3193	2153
1.25	2a	-48.6	1.653	6.342	2910	1699
	2b	-60.0	3.520	6.820	2849	1896
1.50	2a	-30.2	0.860	5.238	2506	1395
	2b	-39.5	2.538	5.674	2405	1576
1.75	2a	-12.4	5.732 ^a	3.800	2236	1023
	2a	-1.3	16.400 ^a	2.270	1909	665
2.00	2a	-7.7	1.544	2.857	1361	836

^a Anomalously high overlap integral because of mixing of π -type orbitals into the BS-OMSOs.

We have stated above that the orbital gap shown in **3** is apparently due to a direct through-space interaction of the oxygen atoms, without significant participation of the hydrogen bridges and have later shown in Figure 5b that the calculated J does not seem to depend on the relative position of the H atoms but on the overlap between the broken-symmetry UMSOs. Such a conclusion is also confirmed by the analysis of the atomic contributions to the overlap between the BS-OMSOs or the BS-UMSOs, since the hydrogen atoms contribute less than 1% of the total overlap. We can thus conclude that the role of the hydrogen bonds in such dimers is essentially structural, that is, they provide the *glue* to hold the two oxygen atoms at a distance in which their atomic orbitals overlap enough to provide an efficient pathway for the exchange interaction.

A nice confirmation of the usually applied qualitative ideas comes from the excellent correlation found between the orbital gap $\epsilon_1 - \epsilon_2$ in the triplet state and the overlap integral (eq 4 for cases **2a** and **2b**), as assumed by Kahn and co-workers for their generic definition of *magnetic* orbitals. Substitution of such an expression in eq 3 would lead to a quadratic dependence of J on the overlap, an alternative form of the Kahn–Briat model.

$$\epsilon_1 - \epsilon_2 = 0.462 + 2767.5 \cdot S_{\text{ab}}(\text{BS-UMSOs}) \quad (\text{in cm}^{-1}; r^2 = 0.994) \quad (4)$$

The J values obtained for compound **A** at different interplanar distances in geometries **2a** and **2b** are plotted as a function of the square of the energy gap between the two OMSOs or between the two UMSOs of the triplet state (Figure 6), and excellent linear fits can be obtained. The point that deviates from the linear behavior in Figure 6 corresponds to the two coplanar monomers, a case in which there is significant mixing of the OMSO with other occupied α orbitals, making the active electron approximation inadequate and has therefore been disregarded for the least-squares fitting. A remarkable result is that the points corresponding to the UMSOs of the two hydrogen-bond geometries explored (**2a** and **2b**) present practically the same trend (eq 5). From the linear fittings in Figure 6 we can obtain estimates for the values of the two-electron terms

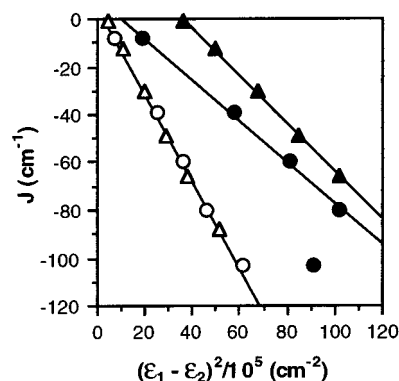


Figure 6. Calculated exchange-coupling constant in the model dimer **1** at different interplanar distances with the H atoms located in the planes of the monomers (**2a**, triangles) or along the O···O vector (**2b**, circles) represented as a function of the square of the energy gap between the two UMSOs (open symbols; regression coefficient $r^2 = 0.998$ for 11 points) or between the two OMSOs (solid symbols) of the triplet state.

K_{ab} and ($J_{\text{aa}} - J_{\text{ab}}$) by comparison with eq 2. The estimated K_{ab} values, $+5.3$, $+36.4$, and $+9.2 \text{ cm}^{-1}$ from UMSOs (of both **2a** and **2b**), OMSOs of **2a** and OMSOs of **2b**, respectively, are rather small compared to those found for, for example, end-on azido, hydroxo, or alkoxo bridges ($+1100$, $+824$, and $+599 \text{ cm}^{-1}$, respectively)^{29,59} and suggest that hydrogen bonding between Cu(II) complexes should not be expected to provide significant ferromagnetic coupling, at least in the presently analyzed molecular topology. The estimated values of ($J_{\text{aa}} - J_{\text{ab}}$), on the other hand (5.51×10^4 , 1.00×10^5 , and $1.16 \times 10^5 \text{ cm}^{-1}$), are similar to those found for other Cu(II) dinuclear complexes with hydroxo, alkoxo,²⁹ oxalato,⁶⁰ oxamidato⁶¹ or 1,3-azido⁵⁸ bridges (between 6.1×10^4 and $1.8 \times 10^5 \text{ cm}^{-1}$)

$$J = 5.32 - \frac{(\epsilon_1 - \epsilon_2)^2}{5.51 \times 10^4} (\text{cm}^{-1}) \quad (\text{from UMSOs}; r^2 = 0.998) \quad (5)$$

Given the good correlations found between J and $(\epsilon_1 - \epsilon_2)^2$, and between $(\epsilon_1 - \epsilon_2)$ and S_{ab} , it comes as no surprise that an excellent linear correlation is found between J and $S_{\text{ab}}(\epsilon_1 - \epsilon_2)$, as suggested by the proposed relationship in eq 3,⁵⁴ or between J and S_{ab}^2 (eqs 6 and 7). If we take the BS-UMSOs to calculate S_{ab} , the term in S_{ab}^2 becomes important for small values of the overlap, contrary to what has been frequently assumed,⁵² whereas the dependence of J on the overlap integral becomes practically linear for large overlap values. It is remarkable that extrapolation of eqs 5–7 (or of the curves in Figure 6) to zero overlap and zero orbital gap consistently gives small K_{ab} estimates (between $+2$ and $+30 \text{ cm}^{-1}$).

$$J = 6.27 - 0.51(\epsilon_1 - \epsilon_2)S_{\text{ab}}(\text{BS-UMSOs}) \quad (\text{in cm}^{-1}; r^2 = 0.999 \text{ for 11 points}) \quad (6)$$

$$J = 7.07 - (1.47 \times 10^4)S_{\text{ab}}^2(\text{BS-UMSOs}) \quad (\text{in cm}^{-1}; r^2 = 0.997 \text{ for 11 points}) \quad (7)$$

(59) Ruiz, E.; Cano, J.; Alvarez, S.; Alemany, P. *J. Am. Chem. Soc.* **1998**, *120*, 11122.

(60) Cano, J.; Alemany, P.; Alvarez, S.; Ruiz, E.; Verdager, M. *Chem. Eur. J.* **1998**, *4*, 476.

(61) Cano, J.; Ruiz, E.; Alemany, P.; Lloret, F.; Alvarez, S. *J. Chem. Soc., Dalton Trans.* **1999**, 1669.

(57) Blanchet-Boiteux, C.; Mouesca, J. M. *Theor. Chem. Acc.* **2000**, *104*, 257.
(58) Fabrizi de Biani, F.; Ruiz, E.; Cano, J.; Novoa, J. J.; Alvarez, S. *Inorg. Chem.* **2000**, *39*, 3221.

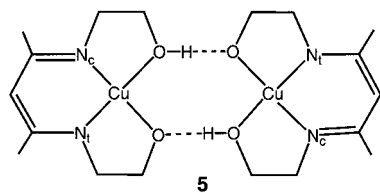
Table 4. NBO Atomic Spin Populations Calculated for Compound **A** and for the Two Isolated Monomers

atom	monomer 1	monomer 2	dimer
Cu	0.5501		0.5862
O(H)	0.0370	0.5506	0.5864
O		0.0371	0.0644
			0.0647
O	0.1562		0.0864
H		0.1566	0.0864
			-0.0012
		0.0024	-0.0012
N _t	0.1511		0.1313
		0.1504	0.1306
N _c	0.0897		0.1212
		0.0899	0.1216

It can thus be concluded that the qualitative models which propose a roughly constant ferromagnetic contribution and an antiferromagnetic contribution dependent on the overlap between two localized magnetic orbitals (or on the associated orbital gap) are consistent with the results of the present DFT calculations, and rather small ferromagnetic contributions (of less than $+30 \text{ cm}^{-1}$) are predicted, regardless of the model used.

Spin Density Distribution

Since there is a general belief that the spin density at the bridging atoms in binuclear complexes should be related to the sign and magnitude of the exchange-coupling constant, we are systematically exploring the spin density distribution in the high-spin state of binuclear complexes.⁶² The most relevant atomic spin populations obtained from our calculations on the triplet state of the molecules studied here are presented in Table 4.



The spin populations in the two monomers are very similar, in keeping with the small differences in their geometries. Although the largest part of the spin density is located at the copper atom, there is an important delocalization of the unpaired electron, mostly to the four donor atoms as found in many transition-metal complexes.⁶² A significant asymmetry in the unpaired electron delocalization can also be detected, with the protonated oxygen much less involved than the unprotonated one. The different involvement of the two oxygen atoms in bonding with Cu is also reflected in the different spin populations at the two N atoms, the one trans to the OH group having a significantly larger spin density than the cis one. The minute participation of the hydrogen atom in the SOMO of the monomer discussed above is appreciated in its rather small positive spin population, which can only be attributed to spin delocalization.

Upon formation of the hydrogen-bonded dimer some interesting changes in the spin populations (calculated for the triplet state) can be appreciated. Despite the asymmetric nature of the hydrogen bond, its formation largely reduces the asymmetry in

the spin population of the two inequivalent oxygen atoms and, consequently, the spin populations of the two N atoms are also much closer to each other. A remarkable effect appears at the hydrogen atoms, which present now a small negative spin population. Such a behavior can be attributed to the combined spin polarization of the O–H bonding electrons and the lone pair of the hydrogen-bonded alkoxo oxygen. Those polarization effects outweigh the very small delocalization of the positive spin of the OMSO toward the hydrogen atom, in contrast with the findings for the monomer, in which only one electron pair affects the spin polarization at the hydrogen atom. With a small enough delocalization of the unpaired electrons toward the hydrogen atoms, spin polarization predominates, and a negative spin population results. Upon asymmetrization of the hydrogen bonds, some contribution may appear, but it is perforce small, compared to that in the lowest SOMO or in the monomers, where there is no nodal plane close to the hydrogen atoms.

Conclusions

The present theoretical studies confirm that hydrogen bonding provides an efficient mechanism for the antiferromagnetic exchange coupling between Cu(II) complexes, provided the hydrogen bonds occur in the plane having the strongest copper–ligand bonds. Such a coupling is due to the through-space overlap of the SOMOs of the two monomers produced by a close contact between the oxygen atoms involved in hydrogen bonding. The exchange-coupling constant is seen to depend on the intermolecular distance or on the interplanar distance, in agreement with orbital overlap criteria, further confirmed by the correlation between the orbital energy gap and the calculated J , as predicted by the Hay–Thibault–Hoffmann orbital model of exchange interactions. Furthermore, it is seen that the coupling constant depends on the square of the overlap integral between the two BS-UMSOs in a linear way, as predicted by the Kahn–Briat model for magnetic orbitals defined in a different way. The different qualitative approaches analyzed are coincident in predicting a small ferromagnetic contribution to the exchange interaction, hence a maximum expected J value of at most $+30 \text{ cm}^{-1}$ for equatorially connected hydrogen-bonded dimers of Cu(II) with topology **1**. Furthermore, our orbital analysis unequivocally confirms that the superexchange interaction in the hydrogen-bonded Cu(II) dimers studied is due to direct through-space interaction between the oxygen atoms of the two monomers, whereas the hydrogen bridges play essentially an indirect structural role by holding those oxygen atoms in close proximity.

A finding that bears some relevance for future theoretical studies is that the empty spin–orbitals of the ferromagnetic case (UMSOs in the present nomenclature) provide a reasonable representation of the corresponding occupied spin–orbitals (OMSOs) in terms of orbital energy gap. Similarly, the unoccupied spin–orbitals of the broken-symmetry state (BS-UMSOs) provide a fair representation of the overlap between the two OMSOs of the same state. Since in many instances the BS-UMSOs present less mixing with lower-lying orbitals and are therefore better localized at the metal d orbitals, the overlap integral between these orbitals provide better correlation with the calculated exchange-coupling constant than the occupied BS-OMSOs.

(62) Cano, J.; Ruiz, E.; Alvarez, S.; Verdager, M. *Comments Inorg. Chem.* **1998**, *20*, 27.

Acknowledgment. The research reported in this paper was boosted by the ESF program on Molecular Magnets and has been supported by the Dirección General de Enseñanza Superior (DGES), Project PB98-1166-C02-01. Additional support from Comissió Interdepartamental de Ciència i Tecnologia (CIRIT) through Grant SGR99-0046 is also acknowledged. The participation of C.D. in this project was initiated thanks to the support of the *Improving the Human Potential Programme, Access to Research Infrastructures*, under Contract HPRI-1999-CT-00071

“Access to CESCO and CEPBA Large Scale Facilities” established between The European Community and CESCO-CEPBA, and was completed within the framework of the program *Improving the Human Research Potential and the Socio-economic Knowledge Base* of the European Commission (Contract HPMF-CT-2000-00977).

JA0178160